JOURNAL OF MATERIALS SCIENCE **34** (1999) 6157–6163

Mechanical anisotropy in the zirconia toughened alumina

M. M. BUĆKO, K. HABERKO
University of Mining and Metallurgy, Faculty of Materials Science and Ceramics, al. Mickiewicza 30, 30-059 Cracow, Poland
E-mail: bucko@uci.agh.edu.pl

The two kinds of the hydrothermally crystallised zirconia powders were used to toughen alumina matrix. The one composed of isometric crystallites of tetragonal symmetry, the other one of elongated monoclinic particles. In the sintered ZTA material either isometric or elongated particles form tetragonal disk shaped inclusions. Zirconia inclusions originating from the elongated particles tend to arrange crystallographically on the uniaxial compaction. This resulted in the material showing different ultrasonic wave velocity, Young modulus, crack lengths and fracture toughness along directions perpendicular and parallel to the compaction force. An explanation of this phenomenon is suggested. Zirconia inclusions originating from the powder composed of isometric crystallites lead to the material of isotropic mechanical properties.

1. Introduction

Usually zirconia toughened alumina (ZTA) shows isotropic mechanical properties [1]. But, in some applications anisotropic properties can be useful. It was shown [2, 3] that the materials of such features could be manufactured by applying the elongated zirconia particles. Such particles crystallise from the hydrous zirconia gel hydrothermally treated in the sodium hydroxide solution [4, 5]. By the same method isometric zirconia particles can also be prepared. But, in this case crystallisation has to be performed in pure water.

The toughening effect in the ZTA materials is related to the tetragonal to monoclinic ($t \rightarrow m$) transformation of zirconia particles incorporated into the alumina matrix [6]. The total free enthalpy change ($\Delta G_{t \rightarrow m}$) caused by this transformation is giving by the expression [7]:

$$\Delta G_{t \rightarrow m} = \Delta G_{chem} + \Delta G_S + \Delta G_E \qquad (1)$$

where: ΔG_{chem} is the free enthalpy change due to the lattice transformation of zirconia. It is the function of temperature and chemical composition. ΔG_S corresponds to the surface energy factor. ΔG_E is the strain energy contribution to the free enthalpy change.

According to [8] the last term can be expressed as:

$$\Delta G_E = \frac{1}{2} \cdot \varepsilon_{ij}^t \cdot \sigma_{ij} \qquad (2)$$

where: σ_{ij}—state of stress around the particle and ε_{ij}^t—is the stress-free strain tensor giving by [9]:

$$\begin{vmatrix} -0.00023 & 0 & 0.08263 \\ 0 & 0.02421 & 0 \\ 0.08263 & 0 & 0.02341 \end{vmatrix}$$

It comes from the equations that the energy absorbed during the transformation is proportional to the strain and stress related to it. So, the greater is the strain the higher should be the toughening effect. It can be concluded from the strain tensor that the largest shear stresses operate along the Z-axis in the vicinity of the transforming monocrystalline zirconia inclusion. The normal stresses along the Y- and Z-axis are close to each other and one order of magnitude greater than along the X direction. So, the highest value of the total stresses should be expected along the Z-axis. This effect should be more pronounced in the case of zirconia particles preferentially elongated towards the Z-axis.

Since the strain caused by the $t \rightarrow m$ transformation of the single zirconia crystal is anisotropic, the toughening effect should depend on the crystallographic orientation of the inclusion. It suggests that the material containing crystallographically oriented zirconia particles should show increased toughness when crack propagates perpendicular to the Z-axis. Fig. 1 illustrates the two extreme orientations of the zirconia particle against the crack. According to the presented discussion in the case "a" the crack arrest should be more effective than in the case "b". In the material containing well arranged zirconia inclusions the anisotropic mechanical properties should be observed.

2. Experimental

Fig. 2 shows the transmission electron micrographs of the zirconia particles applied in the present work. The isometric zirconia particles (Fig. 2a) crystallised from the hydrous zirconia gel hydrothermally treated in distilled water for 2 h at 250 °C. The treatment under the same conditions but in the NaOH water solution of

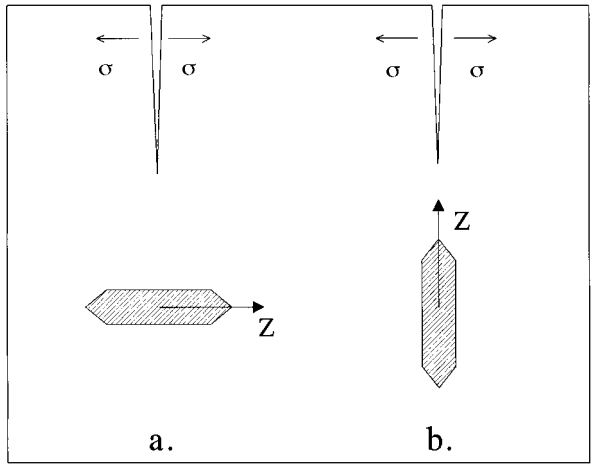

Figure 1 Two extreme orientations of the zirconia particle against the crack.

4 mol/l concentration resulted in the elongated zirconia particles. The α-Al_2O_3 powder was prepared by calcination of the freshly precipitated aluminium hydroxide gel at 1250 °C for 3 h.

X-ray analysis allowed us to determine the phase composition of the zirconia powders by the method described in [10]. The powder composed of isometric crystallites contained 36.6 ± 1.1 vol % of the monoclinic phase, the balance being of tetragonal symmetry. The elongated zirconia particles were totally monoclinic.

Fig. 3 shows the transmission electron micrograph of the elongated zirconia particle and the electron diffraction pattern of the outlined area. The typical pattern for the monocrystal is observed. Fig. 3c presents scheme of the part of the diffraction pattern twisted by the distortion angle (about 60°). Solution of the

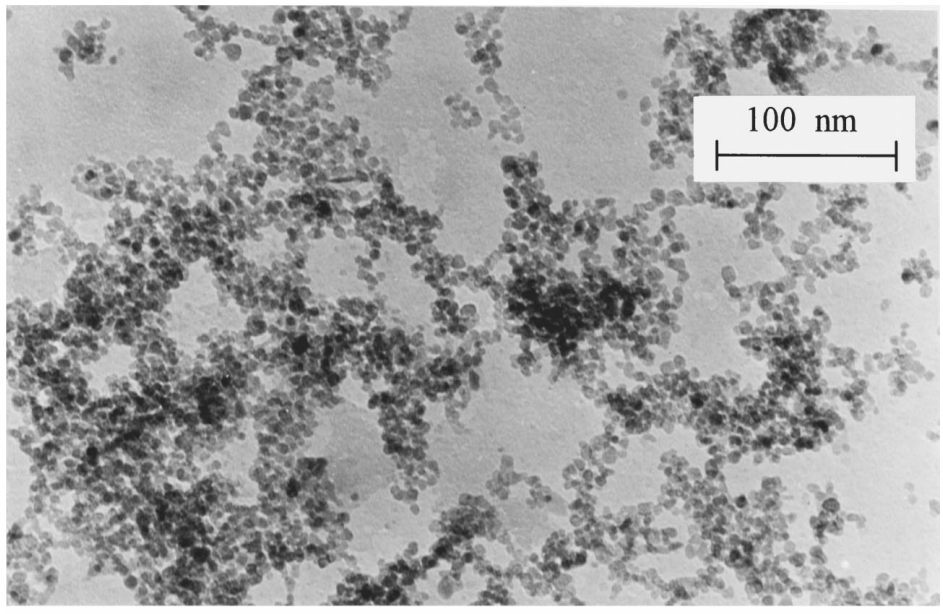

(a)

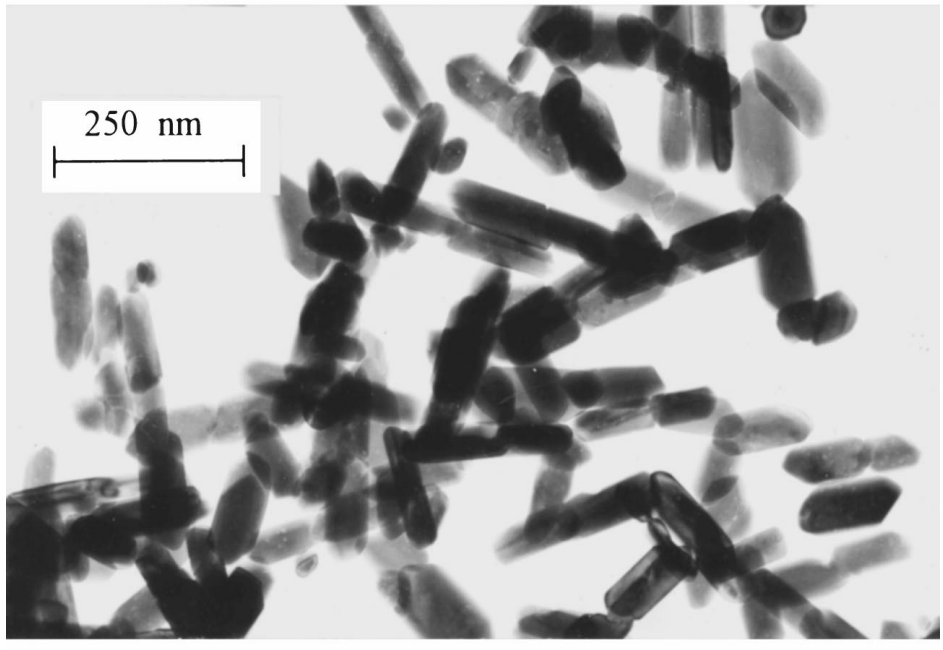

(b)

Figure 2 Morphology of the zirconia powders containing isometric (a) and elongated (b) particles.

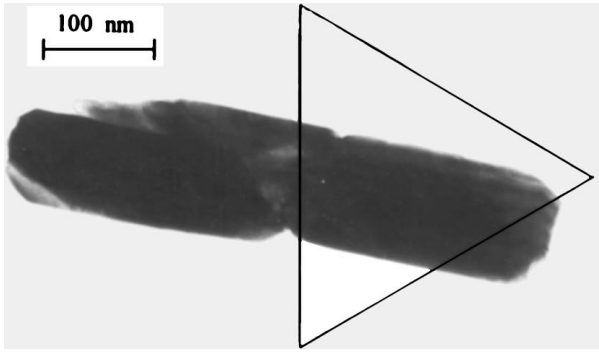

(a)

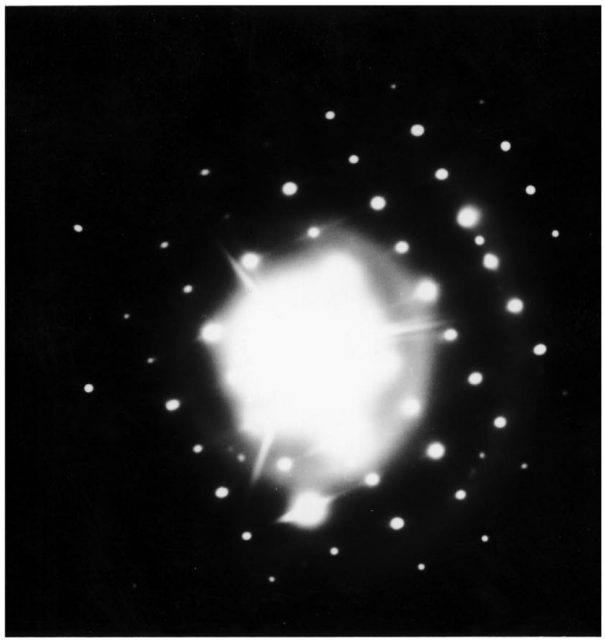

(b)

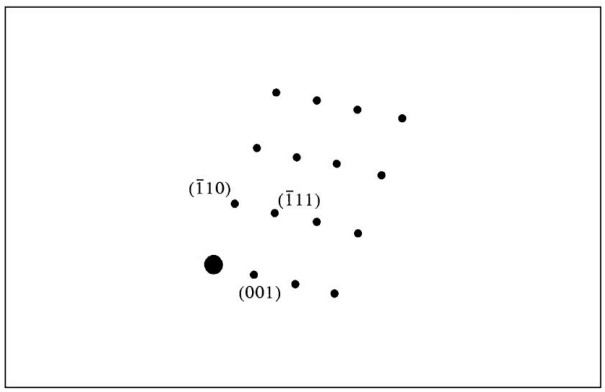

(c)

Figure 3 Transmission electron micrograph of a single zirconia particle (a), electron diffraction pattern from the outlined area (b) and scheme of the part of the diffraction pattern twisted by the distortion angle (c).

diffraction leads to the conclusion that the longer size of the crystal corresponds to the Z-axis of the monoclinic structure. Fig. 4 demonstrates the bright and dark field electron micrographs of the elongated zirconia particles. In the case "a" the angle of lighting was selected in the way satisfying the Bragg condition for the (2 0 0) plain and in the case "b"—this condition was met for the (2 2 0) plane. It is clearly demonstrated in Fig. 4a that the bright faces are parallel to the longer axis of the particle. In Fig. 4b the shining faces, (2 2 0), are also parallel to the longer edges of the particle. Since the Z-axis is the zone axis for the (2 0 0) and (2 2 0) plains, there is no doubt that the monoclinic zirconia particles are elongated along the Z-axis. This conclusion was corroborated by the X-ray peaks intensity analysis of the powder which surface has been subjected to the shear force. Under such conditions the arrangement of the elongated particles parallel to the direction of the applied force is expected. If so, the intensity of the (0 0 2) reflection should be substantially weaker than for the non-arranged particles. Table I demonstrates that this is really the case. This effect does not occur in the case of the powder composed of isometric particles. In order to compare the presented results with the standard values the ICDD data [11] are included.

TABLE I Intensities of the (0 0 2), (0 2 0) and (2 0 0) monoclinic ZrO_2 reflections

Reflection	Powder composed of: Elongated particles	Powder composed of: Isometric particles	Reference intensities
(0 0 2)	8 ± 1	17 ± 1	20
(0 2 0)	9 ± 1	12 ± 1	14
(2 0 0)	22 ± 1	12 ± 1	15

$\pm$ denotes confidence interval at the confidence level of 0.95 throughout the work.

Alumina and zirconia powders (80/20 wt %) were mixed in water at pH $\cong$ 2 fixed with HNO_3, using a ball mill and the alumina grinding media. After 2 h mixing and drying, the powders were uniaxially compacted under 400 MPa. The samples of 26 mm diameter and $\sim$15 mm height were sintered in air atmosphere in an electrically heated furnace at 1700 °C for 2 h. As a reference sample pure alumina sample sintered together with the ZTA materials was applied. The samples containing the elongated zirconia particles additive are referred as "AE", those with isometric ones as "AI" and the pure alumina samples as "A".

3. Results and discussion

Phase analysis of the sintered samples revealed that in the both studied materials containing zirconia the phase of tetragonal symmetry is the dominating one. In the AE sample it corresponds to 87.3 ± 0.9 vol %, and in the AI one, to 96.3 ± 2.1 vol %. It indicates that the majority of the zirconia inclusions have sizes smaller than the critical ones. Densities of all samples were of +98%.

Fig. 5 shows the distribution of the zirconia inclusion surface area in the alumina matrix. It was measured using polished surfaces observed under the scanning electron microscope. The modal values are in the same range of 0.12–0.24 μm^2 corresponding to 0.39–0.55 μm diameter of an equivalent circle. It suggests that a single inclusion is composed of numerous elementary particles no matter of their starting size and shape.

To characterise anisotropy of the green and sintered samples the following features were measured:

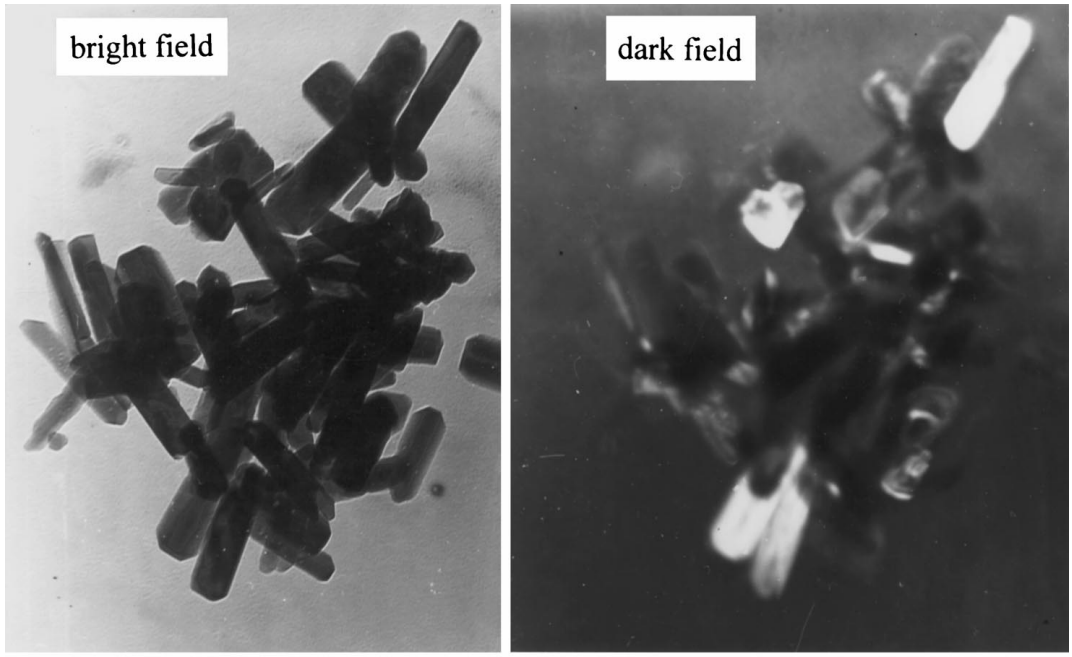

(a)

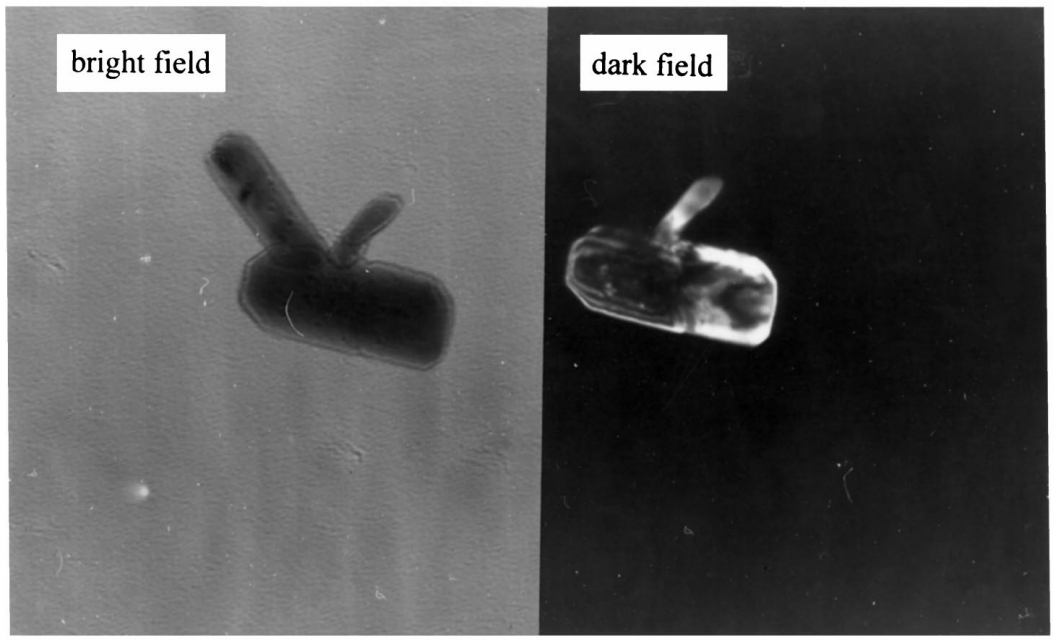

(b)

Figure 4 The bright and dark field electron micrographs of the elongated zirconia particles. Angle of lighting fits the Bragg condition for the (2 0 0) plain (a) and for the (2 2 0) one (b).

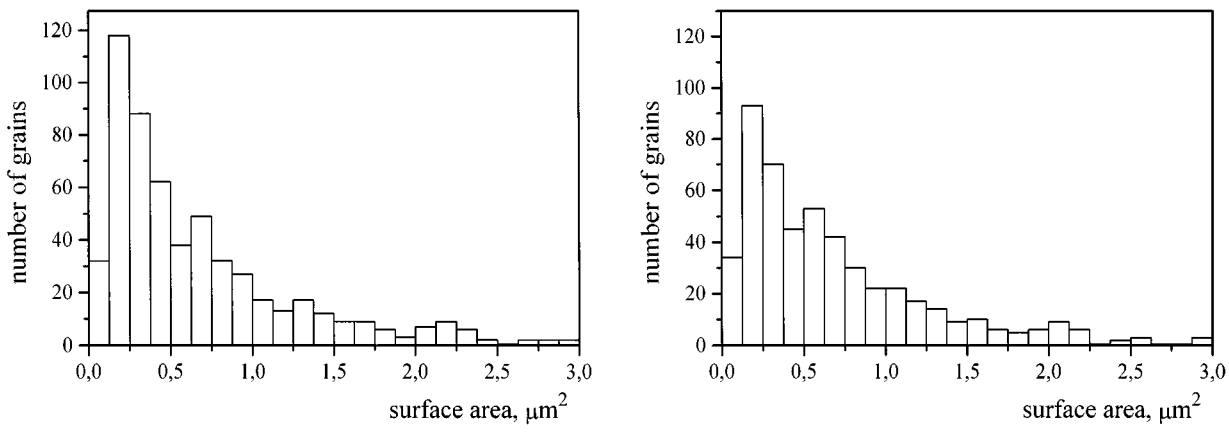

Figure 5 Distributions of the surface area of the zirconia inclusions in the alumina matrix in AE (a) and AI (b) materials, respectively.

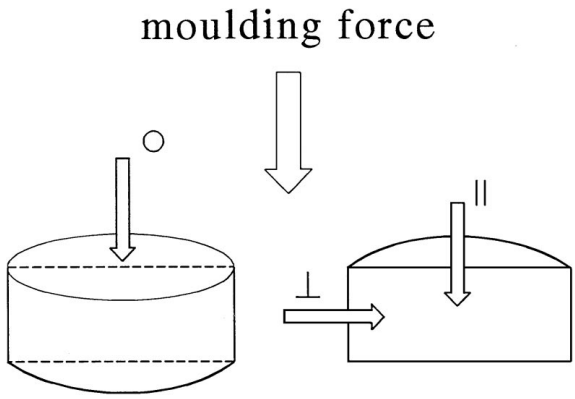

Figure 6 Orientation of the samples.

propagation velocity of the longitudinal ultrasonic waves (10 MHz), length of the cracks caused by the Vicker's indentation and the particle Feret sizes. The X-ray diffraction helped us to gain information on the crystallographic orientation of the zirconia inclusions. All these characteristics were observed in the two perpendicular planes. The first was perpendicular to the direction of the compaction force (marked - **o**) and the second parallel to it (see Fig. 6). In the parallel plane the two directions were distinguished: perpendicular (⊥) and parallel (‖) to this force.

Fig. 7a and b show the zirconia X-ray diffraction peaks in the green AI and AE samples, respectively. According to Fig. 6 they were measured along the specified directions. The evidence of the preferential orientation of the zirconia particles is visible in the AE material; in the surface perpendicular to the compaction force the (0 0 2) reflection (monoclinic) becomes weaker in relation to the (0 2 0) one. It indicates that the starting monoclinic inclusions are arranged with their longer dimension (Z-axis) perpendicular to the compaction force. No such phenomenon occurs in the case of the AI sample (Fig. 7b). It points out that the inclusions composed of isometric crystallites do not arrange crystallographically under the action of the compaction force. The described situation is preserved in the sintered materials. This is illustrated by the date of Table II. The (0 0 2)/(2 2 0) ratio of the tetragonal zirconia reflection intensities in the AI sample shows no dependence on the direction of the moulding force. This is not the case

TABLE II Ratios of the (0 0 2)/(2 2 0) tetragonal reflection intensities in the sintered samples

	Direction		
Material	(‖)	(⊥)	**o**
AE	1.103 ± 0.060	1.121 ± 0.058	0.360 ± 0.046
AI	0.469 ± 0.044	0.463 ± 0.047	0.476 ± 0.041

as for the AE sintered body. It should be notice that no crystallographic orientation within alumina phase occurs in any of the studied systems.

The Feret sizes of the zirconia inclusions were measured along the two perpendicular direction ($d_{\|}$ and $d_{\perp}$) in the plane parallel to the compaction force (Fig. 6). Ratio of these sizes ($d_{\perp}/d_{\|}$) amounted to 1.25 ± 0.46 and 1.38 ± 0.54 for the AE and AI systems, respectively. Statistical evaluation of these figures confirms that they differ essentially from unity. It points out that in the both cases inclusions are disc shaped. Most probably it is due to the deformation of soft zirconia agglomerates under the compaction force. The variance analysis of these size ratios gave evidence that they differ from each other. It indicates that the agglomerates composed of the small, isometric zirconia crystallites reveal higher deformation ability.

Table III shows longitudinal ultrasonic wave velocities measured in the two perpendicular directions. In all green samples wave velocities in the two perpendicular directions differ from each other. These differences are statistically valid. Sintering removes anisotropy of the wave propagation in the pure alumina (A) and in the sample containing isotropic zirconia crystallites (AI). It suggests that the differences of the ultrasonic wave propagation velocities in the green samples should be rather attributed to the disk shaped pores [12] and not to the non-isometric zirconia inclusions. So, the crystallographic orientation of the elongated zirconia inclusions remains as the only factor explaining the behaviour of the sintered AE material. Basing on the longitudinal (V_L) and transverse (V_T) ultrasonic wave velocities Young module (E) along the both distinguished directions in the sintered samples were determined [13]. They are shown in Table III. These data lead to the same conclusions as those presented above.

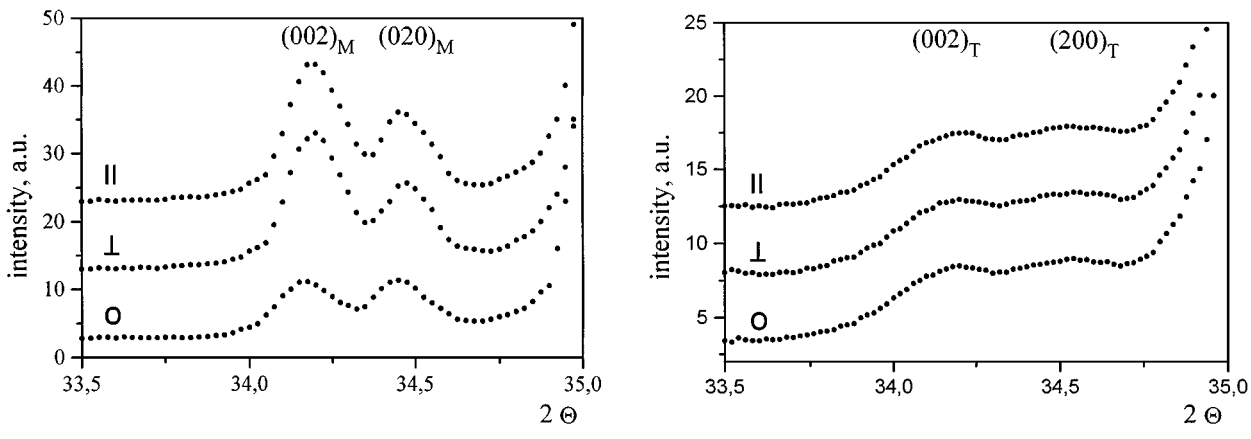

Figure 7 Zirconia X-ray peaks in the green samples AE (a) and AI (b), respectively.

TABLE III Properties of the green and sintered samples of the zirconia toughened alumina

	AE		AI		A	
	Green	Sintered	Green	Sintered	Green	Sintered
V_L, (‖)	922.3 ± 6.9	13452 ± 32	1521.4 ± 8.3	10341 ± 76	1002.6 ± 3.1	11000 ± 20
m/s (⊥)	1278.2 ± 4.2	10584 ± 20	1546.9 ± 4.4	10334 ± 126	1107.7 ± 1.9	10982 ± 58
V_T, (‖)	—	5943 ± 38	—	5901 ± 59	—	6305 ± 97
m/s (⊥)	—	5974 ± 60	—	6050 ± 78	—	6213 ± 58
E, (‖)	—	389 ± 7	—	344 ± 11	—	392 ± 16
GPa (⊥)	—	361 ± 10	—	356 ± 17	—	384 ± 9
L, (‖)	—	157.7 ± 40.2	—	149.9 ± 37.6	—	223.1 ± 54.3
μm (⊥)	—	207.3 ± 46.3	—	148.7 ± 46.4	—	231.5 ± 42.1

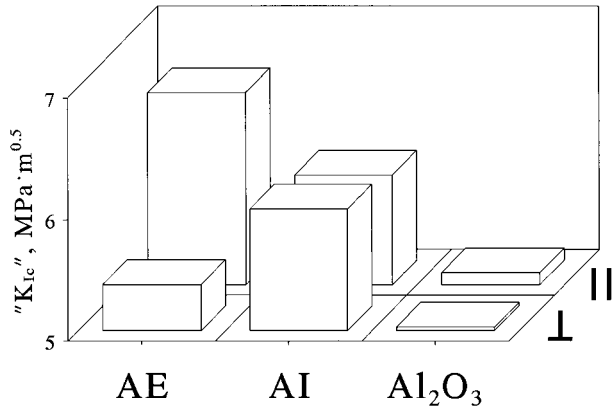

Figure 8 Fracture toughness values, "K_{Ic}", of the ZTA materials.

Cracks provoked by the Vickers indentation were used to assess the toughening effect along the two directions; the one parallel (‖) and the other one perpendicular (⊥) to the direction of the compacting force. These crack lengths (L) are given in Table III. They differ substantially in the case of the AE material. No statistically valid differences occur in the composite containing isometric zirconia crystallites (AI) and in alumina sintered with no additives (A). Using the ultrasonically measured Young module and the crack lengths the K_{Ic} values were calculated on the basis of the Niihara's [14] equation. The data are shown in Fig. 8. As should be expected pure alumina (A) and alumina with isometric zirconia additives (AI) show no differences of the K_{Ic} values along the two distinguished directions. Contrary to this, strong anisotropy occurs in the AE sample. In agreement with the discussion in Section 1 shorter cracks and hence higher "K_{Ic}" value are encountered along the direction parallel to the compaction force, i.e. perpendicular to the Z-axis of the arranged zirconia inclusions. The data of Fig. 8 point out that toughness of the AE material is increased in the direction parallel and decreased in the direction perpendicular to the applied compaction force compared to the AI material. The presented data give clear evidence that the toughening effect is related to the crystallographic arrangement of the zirconia inclusions.

4. Summary

I was shown that by the crystallographic orientation of the zirconia inclusions distributed in the alumina matrix the material of anisotropic mechanical properties could be prepared. Elongated zirconia crystallites have to be used to achieve such result. They arrange on the uniaxial pressing in such a way that their longer axis becomes perpendicular to the compaction force.

It was demonstrated that the zirconia crystallites grow preferentially along the Z-axis when hydrothermally treated in the NaOH solution. Crystallisation in pure water results in the isometric zirconia crystallites. Their application to alumina matrix does not result in a material of anisotropic mechanical properties.

It was found that both kinds of zirconia powders give similar in shape inclusions in the ZTA material; in each case they were disk shaped; they originated from the agglomerates of the starting powders. But, as it was pointed out above, only agglomerates composed of elongated zirconia crystallites lead to the materials of the anisotropic mechanical properties. The necessary condition to obtain the ZTA material of such properties is the crystallographic arrangement of the zirconia crystallites within the inclusions.

Acknowledgement

The authors are grateful to Dr. Jan Piekarczyk for the ultrasonic measurement.

References

1. J. WANG and R. STEVENS, *J. Mater. Sci.* **24** (1989) 3421.
2. M. M. BUĆKO, K. HABERKO, J. PIEKARCZYK and M. FARYNA, in "Third Euro-Ceramics Vol. 3: Engineering Ceramics," Proceedings of the Third European Ceramic Society Conference, Madrid, September 1993, edited by P. Duran and J. F. Fernandez (Faenza Editrice Iberica S.L. 1993) p. 695.
3. M. M. BUĆKO and K. HABERKO, in Proceedings of the Eighth CIMTEC World Ceramics Congress, Vol. 3C: Ceramic Charting the Future, Florence, June 1994 (Techna srl, Faenza, 1995) p. 2077.
4. K. HABERKO, W. PYDA and M. M. BUĆKO, *J. Amer. Ceram. Soc.* **74** (1991) 2622.
5. M. M. BUĆKO, K. HABERKO and M. FARYNA, *ibid.* **78** (1995) 3397.
6. N. CLAUSSEN, *ibid.* **59** (1976) 49.
7. F. F. LANGE, *J. Mater. Sci.* **17** (1982) 225.
8. J. D. ESHELBY, in "Progress in Solid Mechanics," Vol. 2, edited by T. N. Sneddon and R. Hill (Northon-Holland Publisher, Amsterdam, 1961).
9. W. M. KRIVEN, W. L. FRASER and W. S. KENEDY, in "Advances in Ceramics, Vol. 3: Science and Technology of Zirconia II," edited by N. Claussen, M.Rühle and A. H. Heuer (American Ceramic Society, Columbus, 1981).

10. D. L. PORTER and A. H. HEUER, *J. Amer. Ceram. Soc.* **62** (1979) 298.
11. International Centre for Diffraction Date, Powder Diffraction File card 13-307.
12. R. PAMPUCH and J. PIEKARCZYK, "Science of Ceramics," Vol. 8 (The British Ceramics Society, 1976).
13. J. PIEKARCZYK, H. W. HENNICKE and R. PAMPUCH, *Ceram. Forum Int.* **59** (1982) 227.
14. K. NIIHARA, *J. Mater. Sci. Lett.* **2** (1983) 221.

Received 7 September 1997
and accepted 9 March 1999